First-principles calculations of conductance within a plane wave basis set via non-orthogonal Wannier-type atomic orbitals

2006 J. Phys.: Condens. Matter 18 1347

(http://iopscience.iop.org/0953-8984/18/4/019)

INSTITUTE OF PHYSICS PUBLISHING JOURNAL OF PHYSICS: CONDENSED MATTER

J. Phys.: Condens. Matter **18** (2006) 1347–1358 doi:10.1088/0953-8984/18/4/019

First-principles calculations of conductance within a plane wave basis set via non-orthogonal Wannier-type atomic orbitals

Zhenyu Li and D S Kosov

Department of Chemistry and Biochemistry, University of Maryland, College Park, MD 20742, USA

Received 28 October 2005, in final form 30 November 2005
Published 13 January 2006
Online at stacks.iop.org/JPhysCM/18/1347

Abstract

We present a plane-wave/pseudopotential implementation of a method to calculate the electron transport properties of nanostructures. The conductance is calculated via the Landauer formula within the formalism of Green's functions. Non-orthogonal Wannier-type atomic orbitals are obtained by sequential unitary rotations of virtual and occupied Kohn–Sham orbitals, followed by two-step variational localization. We use these non-orthogonal Wannier-type atomic orbitals to partition the Kohn–Sham Hamiltonian into electrode–contact–electrode submatrices. The electrode parts of the system are modelled by two metal clusters with additional Lorentzian broadening of discrete energy levels. We examined our implementation by modelling the transport properties of Na atomic wires. Our results indicate that with the appropriate level broadening the small cluster model for contacts reproduces odd–even oscillations of the conductance as a function of the nanowire length.

(Some figures in this article are in colour only in the electronic version)

1. Introduction

The last decade has witnessed a remarkable miniaturization of conventional microelectronic devices. If this trend is to continue, elements of microelectronic circuits, e.g. transistors and contacts, will soon shrink to the size of a single molecule. One of the major goals in nanotechnology is the construction, measurement and modelling of electronic circuits in which molecular systems act as conducting elements [1, 2]. Accurate and reproducible measurements of current–voltage characteristics have recently been reported for atomic wires and single molecules [3–5]. The experimental progress has been accompanied by considerable advances towards calculations of the transport properties of nanostructures based on density functional theory (DFT). This activity has been largely spurred on by development of several electronic structure codes for first-principles transport calculations [6–9].

The prerequisite for non-equilibrium Green's function calculation of conductance is the partitioning of the Kohn–Sham (KS) Hamiltonian into left/right electrodes and contact regions. Such partitioning is straightforward if one expands the KS wavefunctions as linear combinations of atomic orbitals [6–9] but it becomes a formidable theoretical problem if the plane waves are used for a representation of the KS orbitals. One of the aims of this paper is the development of a theoretical scheme to partition the KS Hamiltonian within a plane-wave basis set.

It has recently been proposed that Wannier functions can be used to link plane-wave electronic structure and Green's function transport calculations [10, 11]. Wannier functions are localized in coordinate space and are obtained by a unitary transformation of the KS orbitals. There are two disadvantages which make standard Wannier functions inapplicable for the calculation of transport properties. First, Wannier functions are defined for occupied KS orbitals and if the same localization scheme is used directly for the virtual orbitals it typically leaves them as delocalized as they were before the unitary transformation. Second, the centres of these localized Wannier functions are not controllable before minimization. To address both issues, we have developed a localization technique which yields non-orthogonal Wannier-type atomic orbitals (NOWAOs) from the plane-wave based KS orbitals. NOWAOs are the maximally localized functions defined via the set of unitary transformations of occupied and virtual KS orbitals. Our scheme is based upon the combination of two localization techniques: Thygesen–Hansen–Jacobsen partially occupied Wannier functions [12] and Mortensen–Parrinello non-orthogonal localization [13]. Combined, these two techniques are used to include the virtual KS orbitals and to shift the Wannier centres from bonds to atoms.

One additional ingredient which is necessary for calculations of conductance is the Green's function of the electrodes. In this paper we represent the leads by two small clusters with additional Lorentzian broadening of the energy levels.

Nanowires of metal atoms have recently attracted much attention because of their fundamental and technological importance. In particular, sodium atomic wire has been studied both experimentally [14–16] and theoretically [17–21]. It was found that the conductance of Na wires exhibits even–odd oscillation as a function of the number of atoms in the wire. The conductance for a wire with an odd number of sodium atoms is close to the quantum of conductance G_0 ($2e^2/h$), while the conductance for a wire with an even number of sodium atoms is less than G_0. Different implementation and junction models lead to different values of the conductance for even-numbered nanowires (0.5–0.9 G_0) [17–21]. We use Na atomic nanowire as a proving ground for our implementation and we aim to reproduce the odd–even oscillation and values of the conductance.

We have implemented the working equations within a plane-wave/pseudopotential code [22] and we will demonstrate the numerical accuracy of implementation for some prototypical test examples. The remainder of the paper is organized as follows. In section 2, we describe the details of our method to calculate the conductance of nanostructures, and its application to sodium atomic wires is given in section 3. In section 4, we conclude the paper.

2. Method

2.1. Partitioning of the Hamiltonian

We begin with the Kohn–Sham equation for the entire nanowire junction

$$H|\psi_i\rangle = E_i|\psi_i\rangle, \tag{1}$$

where H is the Kohn–Sham Hamiltonian and $|\psi_i\rangle$ is the Kohn–Sham orbital. The next step is the partitioning of the system into three parts: two electrodes and wire (typically an atomic

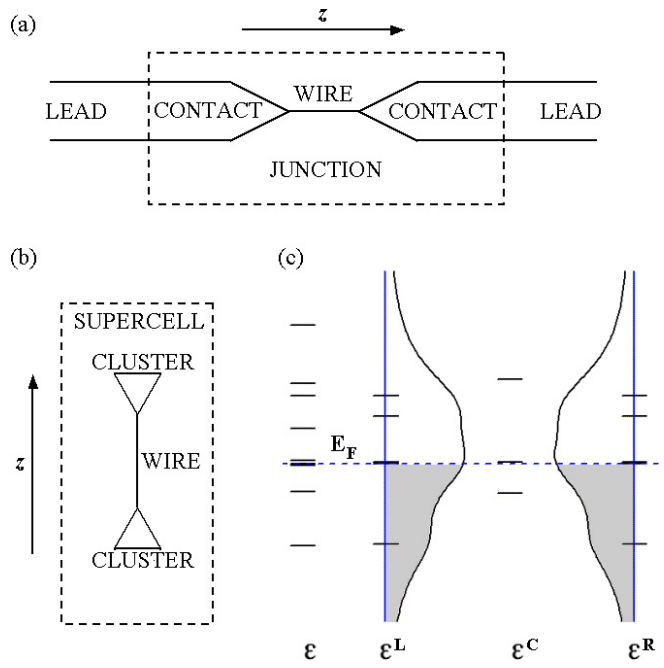

Figure 1. (a) Schematic representation of an atomic/molecular scale junction system for electronic transportation. (b) Simplified transportation model used in our method. (c) Energy levels for a junction system containing a three-atom sodium wire. The density of states obtained by Lorentzian broadening of the electrode levels is also shown. See text for details.

or molecular wire plus parts of the lead) as shown in figure 1. The partitioning of the system results in the partitioning of the Hamiltonian to seven submatrices (left lead, contact, right lead and the lead–wire interactions) and is performed by transforming the representation of the KS Hamiltonian from KS orbitals to atomically localized basis sets:

$$|\psi_i\rangle = \sum U_{\text{in}}|\omega_n\rangle, \tag{2}$$

where U_{in} is a unitary transformation and $|\omega_n\rangle$ form an atomically localized complete basis set. The unitary transformation U_{in} is applied to the KS Hamiltonian

$$H = \sum_i |\psi_i\rangle E_i \langle\psi_i| = \sum_{nm} |\omega_n\rangle H_{nm} \langle\omega_m| \tag{3}$$

with

$$H_{nm} = \sum_i U^*_{ni} E_i U_{im} \tag{4}$$

and yields the partitioning of the Hamiltonian into electrode–wire–electrode submatrices:

$$\mathbf{H} = \begin{pmatrix} \mathbf{H}_{\text{L}} & \mathbf{H}^{\dagger}_{\text{WL}} & 0 \\ \mathbf{H}_{\text{WL}} & \mathbf{H}_{\text{W}} & \mathbf{H}_{\text{WR}} \\ 0 & \mathbf{H}^{\dagger}_{\text{WR}} & \mathbf{H}_{\text{R}} \end{pmatrix}. \tag{5}$$

If the basis set $|\omega_n\rangle$ is not orthogonal, the analogous partitioning should be performed for the overlap matrix $\mathbf{S}$ ($S_{mn} = \langle\omega_m|\omega_n\rangle$). Matrices $\mathbf{H}$ and $\mathbf{S}$ can be defined if indices n and m in H_{nm} (3) are associated with the atomic positions, but this is not the case when periodic boundary conditions are employed and the KS orbitals are expanded in plane waves:

$$\psi_i(\vec{r}) = \frac{1}{\sqrt{\Omega_{\text{cell}}}} \sum_{\vec{G}} C_{i\vec{G}} \exp(\text{i}\vec{G}\vec{r}), \tag{6}$$

where $C_{i\vec{G}}$ are the expansion coefficients. The plane waves $\exp(\mathrm{i}\vec{G}\vec{r})$ do not have any reference to the atomic positions and therefore the partitioning of the KS Hamiltonian into electrode–wire–electrode subspaces cannot be performed directly within the plane-wave representation. Several groups have attempted to overcome this difficulty by using Wannier function representations of the KS orbitals [10, 11].

2.2. Non-orthogonal Wannier-type atomic orbitals

Wannier functions are localized functions which span the same space as the eigenstates of a band or a group of bands. Traditional Wannier functions are obtained by transforming a Bloch representation to a real space representation [23], in which the Bloch vector $\vec{k}$ is substituted by the lattice vector $\vec{R}$ of the unit cell where the orbital is localized:

$$\begin{aligned} |\vec{R}n\rangle &= \frac{\Omega_{\mathrm{cell}}}{(2\pi)^3}\int_{\mathrm{BZ}} |\psi_{n\vec{k}}\rangle \mathrm{e}^{\mathrm{i}\phi_n(\vec{k})-\mathrm{i}\vec{k}\cdot\vec{R}}\,\mathrm{d}\vec{k} \\ &= \frac{\Omega_{\mathrm{cell}}}{(2\pi)^3}\int_{\mathrm{BZ}} \sum_m U_{mn}^{(\vec{k})} |\psi_{m\vec{k}}\rangle \mathrm{e}^{-\mathrm{i}\vec{k}\cdot\vec{R}}\,\mathrm{d}\vec{k} \end{aligned} \tag{7}$$

where $U_{mn}^{(\vec{k})}$ is an arbitrary unitary matrix. The integration in equation (7) is done in reciprocal space within the whole Brillouin zone. The vector $\vec{k}$ equals zero for disordered systems like nanostructures or molecular wire junctions. In this case, the Wannier functions are defined via the unitary transformation of the KS orbitals [24]

$$|\omega_n\rangle = \sum_m U_{mn}|\psi_m\rangle. \tag{8}$$

There are several different schemes for defining the unitary matrix U_{mn} and the choice of unitary transformation can be tailored to particular applications. Finding the maximally localized Wannier functions is pivotal for the partitioning of the Hamiltonian. Although there are several possible ways to define maximally localized Wannier functions, the method of minimization of the mean square spread stands out [25, 26].

Wannier functions are traditionally constructed only from the occupied KS orbitals. Occupied Wannier functions are located on the chemical bonds, which sometimes makes the partitioning of junction systems difficult. The additional complication is that the sum in equation (3) runs over all KS orbitals (occupied and virtual) and due to the completeness requirement it is necessary to consider as many virtual KS orbitals as possible. Therefore, to be used in transport calculations Wannier functions should be constructed in such a way that (a) they are atomically localized and (b) they include both occupied and virtual KS orbitals. The above two requirements are interconnected, since to get atomic centred Wannier functions we must anyway combine unoccupied anti-bonding states with occupied bonding states. The extraction of anti-bonding states from the entire set of virtual orbitals is a difficult computational problem, since unoccupied anti-bonding states are mixed with some scattering states originating from periodic boundary conditions.

Following Thygesen *et al* [12] we begin the localization of the KS eigenstates by constructing a linear combination of the virtual orbitals

$$|\phi_l\rangle = \sum_{m=1}^{N-M} c_{ml}|\psi_{M+m}\rangle, \tag{9}$$

where N is the number of KS orbitals and M is the number of occupied states. Partially occupied Wannier functions are written as [12]

$$|\tilde{\phi}_n\rangle = \sum_{m=1}^{M} U_{mn}|\psi_m\rangle + \sum_{l=1}^{L} U_{M+l,n}|\phi_l\rangle, \tag{10}$$

with L being the number of unoccupied anti-bonding states. The optimal value of L is yet to be determined.

We minimize the following localization functional:

$$\Omega = \sum_n [\langle\tilde{\phi}_n|r^2|\tilde{\phi}_n\rangle - \langle\tilde{\phi}_n|\vec{r}|\tilde{\phi}_n\rangle^2] \tag{11}$$

to choose a suitable unitary transformation U_{mn} and to obtain the maximally localized Wannier functions [25, 26]. For the supercell of the arbitrary symmetry Silvestrelli showed [27] that the minimization of Ω is equivalent to maximization of the functional:

$$\Xi = \sum_n \sum_I w_I |Z^I_{nn}|^2, \tag{12}$$

where matrix $\mathbf{Z}^I$ is defined as

$$Z^I_{mn} = \langle\tilde{\phi}_m|\mathrm{e}^{-\mathrm{i}\vec{G}_I\cdot\vec{r}}|\tilde{\phi}_n\rangle, \tag{13}$$

with $\vec{G}_I$ and w_I being the reciprocal lattice vectors and corresponding weights [24, 27]. For a simple orthorhombic supercell, I ranges from 1 to 3, corresponding to x, y and z, respectively. In practical implementation, $\mathbf{Z}^I$ is calculated by $\mathbf{Z}^I = \mathbf{U}^\dagger\mathbf{Z}^I_0\mathbf{U}$, with $\mathbf{Z}^I_0$ defined as

$$(Z^I_0)_{mn} = \langle\psi_m|\mathrm{e}^{-\mathrm{i}\vec{G}_I\cdot\vec{r}}|\psi_n\rangle. \tag{14}$$

Analytical gradients of the functional Ξ (12) are necessary to perform effective maximization. If we write the unitary matrix at iteration i as $\mathbf{U}_i = \mathbf{U}_{i-1}\exp(-\mathbf{A})$, then the gradients of the functional Ξ with respect to $\mathbf{A}$ can be approximated as

$$(\mathrm{d}\Xi/\mathrm{d}A)_{ij} = \sum_I w_I[Z_{ji}(Z^*_{jj} - Z^*_{ii}) - Z^*_{ij}(Z_{ii} - Z_{jj})]. \tag{15}$$

The gradient with respect to the coefficient matrix c_{lm} is computed by the following formula [12]:

$$\left(\mathrm{d}\Xi/\mathrm{d}c^*\right)_{ij} = \sum_I w_I[[\mathbf{Z_0}\tilde{\mathbf{U}}\mathrm{diag}(\mathbf{Z}^\dagger) + \mathbf{Z_0}^\dagger\tilde{\mathbf{U}}\mathrm{diag}(\mathbf{Z})]\mathbf{U}^\dagger]_{N+i,N+j}, \tag{16}$$

where $\mathrm{diag}(\mathbf{Z})$ is the diagonal part of matrix $\mathbf{Z}$, and $\tilde{\mathbf{U}}$ is the rotation matrix from KS orbitals to partly occupied Wannier functions with dimension $N\times(M+L)$. The orthonormality constraint on matrix $\mathbf{c}$ is invoked through a set of Lagrange multipliers. The steepest descent method is used to maximize Ξ. After the maximization, the unoccupied anti-bonding states are obtained from the coefficient matrix $\mathbf{c}$ through equation (9).

A final set NOWAOs is computed via the additional rotation of partially occupied Wannier functions (10):

$$|\omega_n\rangle = \sum_{m=1}^{M+L} V_{mn}|\tilde{\phi}_m\rangle. \tag{17}$$

The rotation matrix V_{nm} is defined by minimizing the following function [13] independently for each n:

$$\Omega_n = \langle\omega_n|p(\vec{r} - \vec{R}_n)|\omega_n\rangle. \tag{18}$$

The weight function $p(\vec{r})$ is chosen in such a way that it has a minimum at $r = 0$ to localize each $|\omega_n\rangle$ around $\vec{R}_n$. Following Mortensen and Parrinello [13] we select function $p(\vec{r})$ as

$$p(\vec{r}) = \sum_{\alpha=x,y,z}\left[1 - \cos\left(\frac{2\pi}{L}r_\alpha\right)\right]. \tag{19}$$

Ω_n can also be written in the matrix form:

$$\Omega_n = (\mathbf{V}^\dagger \mathbf{P}^{(n)} \mathbf{V})_{nn} = \vec{v}_n^\dagger \mathbf{P}^{(n)} \vec{v}_n, \tag{20}$$

where $\vec{v}_n$ is the nth column of $\mathbf{V}$, and

$$P_{ij}^{(n)} = \langle \tilde{\phi}_i | p(\vec{r} - \vec{R}_n) | \tilde{\phi}_j \rangle \tag{21}$$

with $|\tilde{\phi}\rangle$ being the set of partially occupied Wannier functions obtained by maximization of Ξ. Matrix elements $\mathbf{P}^{(n)}$ are calculated only once and stored for every n. The minimum of Ω_n is obtained when $\vec{u}_n$ is equal to the normalized eigenvector corresponding to the smallest eigenvalue of $\mathbf{P}^{(n)}$. If we need several NOWAOs for a single atomic site, the corresponding number of smallest eigenvectors should be chosen. The number of anti-bonding states necessary for the localization (L in equation (10)) can now be computed by the following formula:

$$L = N_\mathrm{A} N_\mathrm{LE} - M, \tag{22}$$

where N_A is the number of atoms in the system and N_LE is the number of the lowest eigenstates included in the Mortensen–Parrinello localization. For example, for gold atoms, a typical electrode material in molecular electronics, five d-type and one s-type NOWAOs per atom are needed. In figure 2 we plot the generated six NOWAOs for a gold atom in a simple gold wire junction system. We can clearly see that these six NOWAOs reflect the s and d characters of the gold atom.

2.3. Conductance formula

The starting point for the conductance calculations is the Landauer formula [28]

$$G = \frac{2e^2}{h} T(E_\mathrm{F}), \tag{23}$$

where T is the transmission function and E_F is the Fermi energy of the electrodes. Having obtained the partitioned Hamiltonian (5), we can compute transmission as the trace of the Green's function $\mathbf{G}$ and coupling matrices $\mathbf{\Gamma}_{\mathrm{L/R}}$ [8]:

$$T(E) = \mathrm{Tr}[\mathbf{\Gamma}_\mathrm{L}(E)\mathbf{G}(E)\mathbf{\Gamma}_\mathrm{R}(E)\mathbf{G}^\dagger(E)]. \tag{24}$$

The matrices $\mathbf{G}$ and $\mathbf{\Gamma}_{\mathrm{L/R}}$ are expressed by the matrix blocks of the Hamiltonian $\mathbf{H}$, overlap $\mathbf{S}$, self-energy $\mathbf{\Sigma}$

$$\mathbf{G}(E) = [E\mathbf{S}_\mathrm{W} - \mathbf{H}_\mathrm{W} - \mathbf{\Sigma}_\mathrm{L} - \mathbf{\Sigma}_\mathrm{R}]^{-1} \tag{25}$$

and

$$\mathbf{\Gamma}_{\mathrm{L/R}}(E) = \mathrm{i}[\mathbf{\Sigma}_{\mathrm{L/R}} - \mathbf{\Sigma}_{\mathrm{L/R}}^\dagger]. \tag{26}$$

The self-energies $\mathbf{\Sigma}_{\mathrm{L/R}}$ are defined via the Green's function of the left and right electrodes $\mathbf{g}$ and the electrode–wire interactions:

$$\mathbf{\Sigma}_{\mathrm{L/R}}(E) = (E\mathbf{S}_{\mathrm{WL/R}} - \mathbf{H}_{\mathrm{WL/R}})\mathbf{g}_{\mathrm{L/R}}(E)(E\mathbf{S}_{\mathrm{WL/R}}^\dagger - \mathbf{H}_{\mathrm{WL/R}}^\dagger). \tag{27}$$

It is not possible to include the whole of the leads in the practical calculations. The interaction between the wire and the infinitely large leads is accounted for by the self-energy. Different theoretical models have been proposed to obtain $\mathbf{g}$. The most accurate schemes rely on the surface Green's function method. Even with some special techniques, such as the transfer matrix [29, 30] and decimation techniques [31], the computation of the surface Green's function is complex and time-consuming. Since detailed experimental geometrical structures of the leads and nanowire are unclear in most cases, this enables us to use the simpler models for

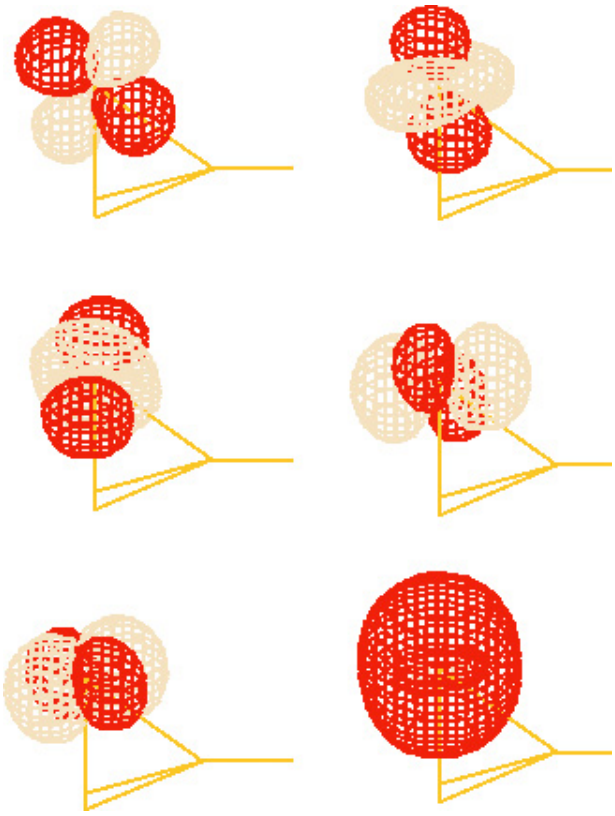

Figure 2. Non-orthogonal Wannier-type atomic basis functions for one gold atom in a simple gold junction system. Only half of the junction is shown.

the leads. In this paper the electrode is represented by a metal cluster with additional energy level broadening [32]. This model has proved to be very successful in estimation of the bulk density of states from small cluster calculations [33, 34]. The Lorentzian broadening σ in the electrode density of states is equivalent to positive infinitesimal σ in the electrode Green's function:

$$\mathbf{g} = [(E + \mathrm{i}\sigma)\mathbf{S}_{\mathrm{L/R}} - \mathbf{H}_{\mathrm{L/R}}]^{-1}. \tag{28}$$

Sai *et al* [35] have recently demonstrated that the static DFT calculations overestimate the electric current and it can be corrected by adding the term $\sim \int \mathrm{d}z\, \eta(\partial_z \rho)^2/\rho^4\, \mathrm{d}z$ to the resistance, where η is the zero-frequency limit of the electron viscosity and ρ is the electron density. These corrections can be readily included into our calculations, but for the examples considered in this paper (Na wires) they can be neglected since the variations of electron density along the wire axis are small [35]. The gradient of the density becomes substantial for molecular wire junctions and may result in large corrections.

3. Test results

3.1. Computational methods

To illustrate the performance of our method we computed the transport properties of Na nanowire. The calculations were performed using our implementation of the formalism

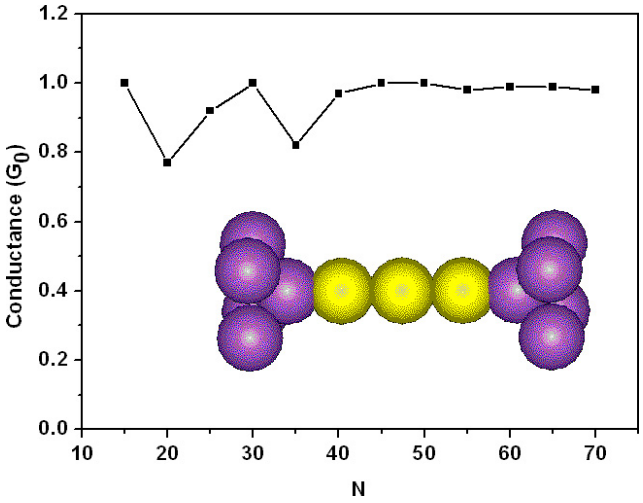

Figure 3. Conductance of a three-atom Na atomic wire as a function of the number of Kohn–Sham orbitals calculated to construct the NOWAOs. The Kohn–Sham orbitals are computed for a complete electrode–wire–electrode system and the electrodes are modelled by five-atom clusters. The inset shows the geometry of this junction system.

presented here in the CPMD package [22]. All systems were treated employing periodic boundary conditions and the KS orbitals were expanded in plane waves (50 Ryd cut-off) at the Γ point of the Brillouin zone. We used local density approximation for the exchange and correlation functional and Stumpf, Gonze and Schettler pseudopotentials [36] for core electrons. The system is simulated by a cluster in a large supercell. The size of the supercell is chosen in such a way that the distance between the nearest atoms in the neighbouring cells is larger than 8.5 Å, so that the interaction between supercell images is negligible. An extensive set of the KS virtual orbitals is computed via Lanczos diagonalization [37] to ensure that all possible unoccupied anti-bonding states are included. To speed up convergence of the self-consistent iterations, a free energy functional [38] is used with the electronic temperature $T = 300$ K. Since sodium is a single-valent atom, only one NOWAO per Na atom is constructed from the KS orbitals.

The whole system is divided into three parts: left electrode, central wire and right electrode. The electrode part is obtained by cutting a few atoms from the Na(001) surface. In particular, as shown in the inset of figure 3, we cut a five-atom cluster, which is composed of a square four-atom base and an apical atom. The geometry of this five-atom cluster is fixed to the bulk values. The wire part is a single chain of Na atoms, where the distance between the atoms is constrained to the nearest neighbour distance in the bulk system. The distance between the electrode part and the wire part is optimized. The optimized value d is listed in table 1 and it shows small $\sim$0.1–0.2 Å odd–even oscillation as the length of the wire varies. We use the optimized value of electrode–wire separation in all our calculations.

Let us take a three-atom Na wire as an example to illustrate conductance calculations by the method we described in the previous section.

First, the electronic structure of the whole system is calculated and a set of KS orbitals is obtained. The number of KS orbitals should be large enough to include all unoccupied anti-bonding states. Figure 3 shows the conductance as a function of the number of KS orbitals included in the localization procedure to define NOWAOs. The deviation of the conductance

Table 1. Distance between electrode and wire d (in Å), and conductance of the Na atomic wire junction systems. The length of the Na wire N ranges from two to five atoms. The electrode part of the junction system is modelled by one (E1 model) or five (E5 model) Na atoms. Conductances for four different broadening parameters 0.02, 0.025, 0.03, and 0.04 Hartree are listed. See text for more details.

	E1 model					E5 model				
N	d	0.02	0.025	0.03	0.04	d	0.02	0.025	0.03	0.04
2	3.004	0.33	0.43	0.50	0.57	3.078	0.64	0.71	0.75	0.77
3	3.070	0.99	0.99	0.98	0.97	3.270	0.99	1.00	1.00	0.99
4	3.024	0.65	0.81	0.92	1.00	3.097	0.71	0.72	0.72	0.69
5	3.042	0.99	0.99	0.99	0.99	3.221	1.00	1.00	0.98	0.96

from the correct value (1 G_0) vanishes rapidly as the number of virtual KS orbitals is increased. Our test calculations illustrate that the number of virtual KS orbitals can be adjusted to achieve any desired level of accuracy in the conductance calculations. The results in figure 3 demonstrate that 45 virtual KS orbitals are sufficient to get the converged result for a three-atom Na wire.

Second, this set of KS orbitals is used to construct NOWAOs, with which the Hamiltonian matrix **H** and the overlap matrix **S** are calculated. By solving the corresponding generalized eigenvalue problem we get a set of energy levels ϵ for the whole junction system, as shown in the left column of figure 1(c). The differences between these eigenlevels and the Kohn–Sham energies are very small, especially for occupied states. At the same time, partition of **H** and **S** is implemented, and the energy levels of the electrodes, ϵ^{L} and ϵ^{R}, are obtained by solving the generalized eigenvalue problem for the corresponding submatrices.

Third, we introduce Lorentzian broadening of the left and right energy levels to continuous density of states, to compute the self-energy matrices. The broadening parameter σ is chosen to be 0.025 Hartree here, and the effect of the broadening parameter on conductance will be discussed later. The transmission probability is computed by using the equations in section 2.2. The peak positions of the transmission curve can be considered as renormalized eigenlevels of the central three-atom Na wire coupled to the electrodes (ϵ^{C} in figure 1).

In units of G_0, the conductance equals the value of the transmission at the Fermi energy of the leads. The Fermi energy for the electrode is not known *a priori* and it has to be computed within the approach. The Fermi energy is rigorously defined as the energy at which the integrated density of states is equal to the number of electrons in the electrode cluster [32]. The charge population of the electrode cluster is calculated by $\rho_{\mathrm{L/R}} = \sum_{i\in \mathrm{L/R}} (\mathbf{S}^{1/2}\mathbf{P}\mathbf{S}^{1/2})_{ii}$, where **P** is the density matrix on the NOWAOs basis set, which is obtained from the generalized eigenvalue problem of the whole junction cluster system. We found out that if one uses very small clusters to represent the electrodes this method of Fermi energy calculations leads to a significant dependence of the Fermi energy on the value of the electrode level broadening. Therefore in our calculations we set the Fermi energy of the electrodes to the position of the Fermi energy of the complete electrode–wire–electrode system. This is justified for our particular system since the electrodes and the wire are built from the same atoms. When the electrode clusters are very large, the Fermi energy of the complete system becomes the same as the Fermi energy of the electrodes computed via the integration of the density of states.

3.2. Oscillation of conductance

The most important feature of electronic current flow through Na atomic wires is that the conductance oscillates as a function of the number of atoms in the wire. We calculate the

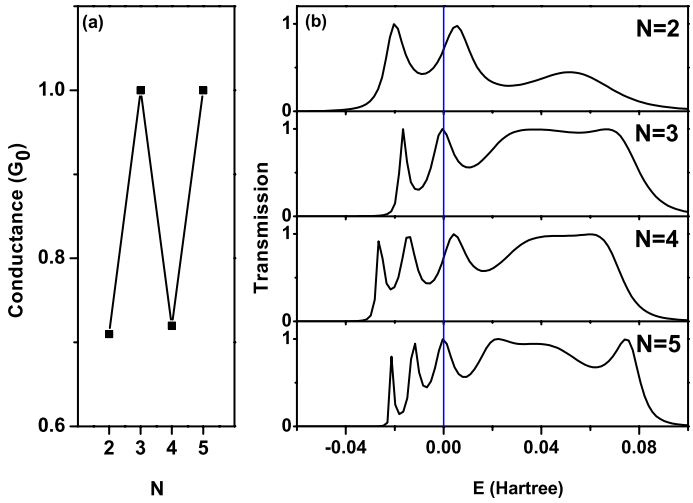

Figure 4. (a) Conductance oscillation of sodium atomic wire with its length. (b) Transmission curves of the sodium atomic wires. The Fermi energy is set to zero.

conductance of Na atomic wires with a length range from two to five atoms. The odd–even oscillation of the conductance is well reproduced as shown in figure 4(a). The conductance for $N = 3$ and 5 is one unit conductance G_0, while the conductance for $N = 2$ and 4 is about 0.7 G_0. The transmission curves for these wire systems are plotted in figure 4(b). We can see that the number of sharp peaks in the transmission curves, i.e. the number of resonant states, is equal to the number of atoms in the wire. The low-temperature transport properties are mainly determined by the states near the Fermi energy. There is a resonant state at the Fermi energy for odd-numbered Na wires, but there is no such state for even-numbered Na wires. This is exactly the reason for the even–odd oscillation behaviour of the conductance [18, 20].

3.3. Eigenchannels

Since there are multiple peaks in the transmission curve, it is interesting to see if sodium wires are single channel conductors as we expected for monovalent atomic chains. By defining

$$\mathbf{t} = \mathbf{\Gamma}_{\mathrm{L}}^{\frac{1}{2}} \mathbf{G}^{\mathrm{R}} \mathbf{\Gamma}_{\mathrm{R}}^{\frac{1}{2}} \tag{29}$$

the transmission can be written as $T(E) = \mathrm{Tr}(\mathbf{t}\mathbf{t}^{\dagger})$. We can decompose the transmission to the combination of some eigenchannels diagonalizing the matrix $\mathbf{t}\mathbf{t}^{\dagger}$ [39]. For sodium wires, we get only one non-zero eigenvalue at any energy, which is the manifestation of a single-channel conduction mechanism.

3.4. Electrode cluster model

In our method the electrode is approximated by a small cluster with proper level broadening. Therefore it is important to understand how the results of our calculations are affected by the cluster size and by the choice of the broadening.

The size of the electrode cluster should be big enough so that charge neutrality is maintained for the junction system. As discussed in the sections 3.1 and 3.2 the five-atom

electrode model is sufficient to simulate the transport behaviour of sodium wires in our method[1]. This is already a very small size in comparison with typically used models for electrodes, but it is interesting to see if a smaller cluster still works in our method. For this purpose we also check the simplest one-atom model. The results are listed in table 1. Compared with the five-atom model, the oscillation strength of the optimized distance between the electrode and wire is smaller. We can see that the conductance for the one-atom model still exhibits the even–odd oscillation, but the conductance of even-numbered wires is not very stable anymore. This result indicates that the one-atom electrode model provides an oversimplified description of the system.

It is also important to test whether the broadening parameter strongly affects the results of the transport calculations. We analysed the conductances for all wires by varying the broadening parameter σ from from 0.02 to 0.04 Hartree, and list the results in table 1. We find that for the large electrode model the conductance is not very sensitive to the variations of σ, especially for an odd-numbered wire system. For the one-atom electrode model, the conductance changes significantly as σ varies. This is because there is only one electrode energy level for the one-atom model, and the shape of the density of states at E_{F} strongly depends on the broadening parameter.

There is another method for calculating the conductance for a single-channel nanowire [18, 40]. It is based on the Friedel sum rule and also relies on the eigenlevel broadening technique to represent the continuum of states in the contact. In that method, the eigenvalues of the whole junction system ϵ are broadened to obtain the density of states, thus the broadening parameter should be smaller than the resonance spacing but larger than the single particle level spacing for the electrode. To satisfy this constraint, the spacing of ϵ^{L} and ϵ^{R} should be much smaller than that of ϵ^{C}, and therefore much larger electrode clusters should be used in calculations based on the Friedel sum rule. In our method, however, if the broadening parameter is comparable to the resonance spacing we still get very accurate results. Therefore, much smaller metal clusters can be used to model electrodes within our implementation.

4. Conclusions

We have developed and implemented a plane-wave based method to calculate the conductance of nanostructures. The fundamental quantities in the present implementation are NOWAOs which are obtained by the multistep localization of KS orbitals. NOWAOs are used to partition KS Hamiltonian to electrode–wire–electrode submatrices that is a necessary step for the Green's function based conductance calculations. The electrode parts are modelled by small clusters with proper broadening of their eigenlevels, and this model is especially suitable for systems for which we have a very limited knowledge of the lead–wire bonding structure. Transport properties of sodium nanowires are studied by this method and the odd–even oscillations of the conductance are reproduced.

Acknowledgments

The authors are grateful to F Evers, M Gelin and K S Thygesen for helpful discussion. This work was partially supported by the Mitsubishi Chemical Corporation.

[1] We have also tested the 10-atom cluster model, which is obtained by adding another layer to the electrode from the Na(001) surface. With smaller broadening parameters, the bigger model gives similar results to the five-atom cluster model discussed in the text.

References

[1] Bowler D R 2004 *J. Phys.: Condens. Matter* **16** R721
[2] Nitzan A and Ratner M A 2003 *Science* **300** 1384
[3] Reed M A, Zhou C, Muller C J, Burgin T P and Tour J M 1997 *Science* **278** 252
[4] Cui X D, Primak A, Zarate X, Tomfohr J, Sankey O F, Moore A L, Moore T A, Gust D, Harris G and Lindsay S M 2001 *Science* **294** 571
[5] Xu B and Tao N J 2003 *Science* **301** 1221
[6] Taylor J, Guo H and Wang J 2001 *Phys. Rev.* B **63** 245407
[7] Brandbyge M, Mozos J-L, Ordejon P, Taylor J and Stokbro K 2002 *Phys. Rev.* B **65** 165401
[8] Xue Y, Datta S and Ratner M 2002 *Chem. Phys.* **281** 151
[9] Evers F, Weigend F and Köntopp M 2004 *Phys. Rev.* B **69** 235411
[10] Calzolari A, Mazari N, Souza I and Nardelli M B 2004 *Phys. Rev.* B **69** 35108
[11] Thygesen K S and Jacobsen K W 2005 *Chem. Phys.* **319** 111
[12] Thygesen K S, Hansen L B and Jacobsen K W 2005 *Phys. Rev. Lett.* **94** 26405
[13] Mortensen J J and Parrinello M 2001 *J. Phys.: Condens. Matter* **13** 5731
[14] Krans J M, van Ruitenbeek J M, Fisun V V, Yanson I K and de Jongh L J 1995 *Nature* **375** 767
[15] Krans J M, van Ruitenbeek J M and de Jongh L J 1996 *Physica* B **218** 228
[16] Yanson A I, Yanson I K and van Ruitenbeek J M 1999 *Nature* **400** 144
[17] Lang N D 1997 *Phys. Rev. Lett.* **79** 1357
[18] Sim H-S, Lee H-W and Chang K J 2001 *Phys. Rev. Lett.* **87** 96803
[19] Tsukamoto S and Hirose K 2002 *Phys. Rev.* B **66** 161402
[20] Lee Y J, Brandbyge M, Puska M J, Taylor J, Stokbro K and Nieminen R M 2004 *Phys. Rev.* B **69** 125409
[21] Khomyakov P A and Brocks G 2004 *Phys. Rev.* B **70** 195402
[22] CPMD V3.9 Copyright IBM Corp 1990–2004, Copyright MPI fuer Festkoerperforschung Stuttgart 1997–2001
[23] Wannier G H 1937 *Phys. Rev.* **52** 191
[24] Berghold G, Mundy C J, Romero A H, Hutter J and Parrinello M 2000 *Phys. Rev.* B **61** 10040
[25] Marzari N and Vanderbilt D 1997 *Phys. Rev.* B **56** 12847
[26] Souza I, Marzari N and Vanderbilt D 2002 *Phys. Rev.* B **65** 35109
[27] Silvestrelli P L 1999 *Phys. Rev.* B **59** 9703
[28] Datta S 1997 *Electronic Transport in Mesoscopic Systems* (Cambridge: Cambridge University Press)
[29] Lee D H and Joannopoulos J D 1981 *Phys. Rev.* B **23** 4988
[30] Lee D H and Joannopoulos J D 1981 *Phys. Rev.* B **23** 4997
[31] Lopez Sancho M P, Lopez Sancho J M and Rubio J 1985 *J. Phys. F: Met. Phys.* **15** 851
[32] Tada T, Kondo M and Yoshizawa K 2004 *J. Chem. Phys.* **121** 8050
[33] Lee K, Callaway J and Dhar S 1984 *Phys. Rev.* B **30** 1724
[34] Zhao J, Yang J and Hou J G 2003 *Phys. Rev.* B **67** 85404
[35] Sai N, Zwolak M, Vignale G and Di Ventra M 2005 *Phys. Rev. Lett.* **94** 186810
[36] Gonze X, Stumpf R and Scheffler M 1991 *Phys. Rev.* B **44** 8503
[37] Pollard W T and Friesner R A 1993 *J. Chem. Phys.* **99** 6742
[38] Alavi A, Kohanoff J, Parrinello M and Frenkel D 1994 *Phys. Rev. Lett.* **73** 2599
[39] Brandbyge M, Sorensen M R and Jacobsen K W 1997 *Phys. Rev.* B **56** 14956
[40] Datta S and Tian W 1997 *Phys. Rev.* B **55** R1914